Convective Lyapunov spectra

2013 J. Phys. A: Math. Theor. 46 254013

(http://iopscience.iop.org/1751-8121/46/25/254013)

IOP PUBLISHING JOURNAL OF PHYSICS A: MATHEMATICAL AND THEORETICAL

J. Phys. A: Math. Theor. **46** (2013) 254013 (10pp) doi:10.1088/1751-8113/46/25/254013

Convective Lyapunov spectra

Aurélien Kenfack Jiotsa[1,2], Antonio Politi[2,3] and Alessandro Torcini[2,4,5]

[1] Département de Physique, Ecole Normale Supérieure, Université de Yaoundé I, BP 42 Yaoundé, Cameroon
[2] Istituto dei Sistemi Complessi, Consiglio Nazionale delle Ricerche, via Madonna del Piano 10, I-50019 Sesto Fiorentino, Italy
[3] Institute for Complex Systems and Mathematical Biology, King's College, University of Aberdeen, Aberdeen AB24 3UE, United Kingdom
[4] Centro Interdipartimentale per lo Studio delle Dinamiche Complesse, via Sansone 1, I-50019 Sesto Fiorentino, Italy
[5] INFN Sez. Firenze, via Sansone 1, I-50019 Sesto Fiorentino, Italy

E-mail: a.politi@abdn.ac.uk

Received 12 November 2012, in final form 19 March 2013
Published 4 June 2013
Online at stacks.iop.org/JPhysA/46/254013

Abstract
We generalize the concept of the convective (or velocity-dependent) Lyapunov exponent from the maximum rate $\Lambda(v)$ to an entire spectrum $\Lambda(v, n)$. Our results are derived by following two distinct computational protocols: (i) Legendre transform within the chronotopic approach (Lepri *et al* 1996 *J. Stat. Phys.* **82** 1429); (ii) by letting evolve an ensemble of initially localized perturbations. The two approaches turn out to be mutually consistent. Moreover, we find the existence of a phase transition: above a critical value $n = n_c$ of the integrated density of exponents, the zero-velocity convective exponent is strictly smaller than the corresponding Lyapunov exponent. This phenomenon is traced back to a change of concavity of the so-called *temporal* Lyapunov spectrum for $n > n_c$, which, therefore, turns out to be a dynamically invariant quantity.

This article is part of a special issue of *Journal of Physics A: Mathematical and Theoretical* devoted to 'Lyapunov analysis: from dynamical systems theory to applications'.

PACS number: 05.45.−a

(Some figures may appear in colour only in the online journal)

1. Introduction

The linear stability analysis of a chaotic state is performed by computing as many Lyapunov exponents (LEs) $\{\lambda_l\}$ as the number N of variables of the corresponding dynamical system. One commonly refers to the LEs ordered from the largest to the most negative one as the *Lyapunov spectrum*. In a one-dimensional lattice of coupled dynamical systems, $N = Ld$, where L is the lattice length and d the number of variables per lattice site ($d = 1$ in the case of logistic maps, while $d = 3$ if the dynamical systems are either Rössler or Lorenz attractors). If the system size is large enough ($L \gg 1$), then the Lyapunov spectrum is a function of the integrated density $n = l/L$, i.e. $\lambda_l = \lambda(n = l/L)$ [1]. It is customary to interpret this scaling behaviour as the evidence of extensivity of the chaotic dynamics in spatial systems. Lyapunov spectra, although providing a detailed characterization of the stability of generic infinitesimal perturbations do not help to describe their spatial propagation. The convective (comoving) Lyapunov exponent (CLE) $\Lambda(v)$ was introduced in [2], precisely to quantify the (maximal) growth rate of an initially localized perturbation in a frame that moves with a velocity v. Later, it was recognized that the CLE can be derived from the general *chronotopic* approach [3]. Starting from the evolution of infinitesimal perturbations along generic space–time directions, this method leads to the conjecture that all the stability properties of one-dimensional systems are encoded into the so-called *entropy potential*, a function of the spatial and temporal growth rate of a generic perturbation. In the context of this paper, one is interested in the growth rate $\lambda(n, \mu)$ (the so-called *temporal* Lyapunov spectrum [3]) of a perturbation with a spatially exponential profile $\exp(-\mu i)$, where i denotes a discrete spatial variable and μ is a free parameter. In [4], it was shown that the CLE $\Lambda(v)$ can be obtained by Legendre transforming $\lambda(0, \mu)$.

In systems with left–right spatial symmetry, $\Lambda(v)$ is symmetric around $v = 0$, where it attains its maximum value which coincides with the standard maximum LE. The largest velocity $v = v_c$ such that $\Lambda(v) \geqslant 0$ is the maximal propagation velocity of infinitesimal perturbations. In convectively unstable systems, $\Lambda(0) < 0$ and the (positive) maximum convective exponent is attained for some nonzero velocity. A somehow similar approach was developed by Huerre and Monkewitz [5] to characterize absolute and convective instabilities in open flows and more recently extended by Sandstede and Scheel to deal with generic boundary conditions [6].

The CLE quantifies the local growth rate of the *amplitude* of a generic perturbation, but does not provide any information on the way different *volumes* tend to locally fill the available space. In this paper, we give an answer to such a question. The chronotopic approach offers a natural way to determine an entire spectrum of *convective* LEs, by implementing the Legendre transform for a generic value of the integrated density n (i.e. for $n \neq 0$). It would be, however, desirable to give a more direct definition as well. In principle, the most appropriate starting point for a direct definition of a spectrum of CLE is the approach developed in [7], where an ensemble of linearly independent initial conditions (localized within a window of size L) was freely let evolve to thereby determine volume expansion rates within the very same window. As a result, it was noted that meaningful generalized LEs could be defined by simultaneously letting the time T and the size L tend to infinity, with a constant ratio $g = T/L$. The standard Lyapunov spectrum is recovered for $g \to 0$, while in the opposite limit $g \to \infty$, all exponents coincide with the maximum. The dependence on g expresses the fact that the growth along different directions is affected in a different manner by the local expansion and by diffusion. In principle, this approach can be implemented for moving windows, too; the unavoidable dependence on the additional parameter g reduces, however, the appeal of such a direct method. Accordingly, we have preferred to sacrifice the appeal of an impeccable definition in favour of the implementation of a less direct, but operative protocol. In practice, we complement the moving-window approach with suitable boundary conditions to get rid of the difficulty of dealing with an open system (note that this is the setup proposed in [8]).

In this paper, we show that the spectrum of CLEs obtained with the latter approach is consistent with that obtained by means of the above-mentioned Legendre transform. This confirms that the chronotopic approach 'encodes' all the linear stability properties of one-dimensional spatio-temporal systems [3]. Moreover, the chronotopic approach is by and large more accurate and this allows discovering serious numerical difficulties that easily lead to artefacts, when the Lyapunov spectra are blindly computed by implementing the direct method (even in the simple case of coupled one-dimensional maps, herein investigated). Moreover, the chronotopic approach reveals the existence of a phase transition: above a critical value n_c of the integrated density n, the zero-velocity CLE does no longer coincide with the standard LE (for the same value of n). This phenomenon is mathematically ascribable to a change of concavity in the temporal Lyapunov spectrum. We conjecture that the physical motivation is that convective phenomena become much stronger than diffusion, weakening the local growth of typically uniform perturbations. Finally, note that n_c is a dynamically invariant dimension-density such as that of the unstable manifold and of the attractor itself (through the Kaplan–Yorke formula). Its direct physical meaning needs, however, to be clarified.

In the following section, we introduce the model and the general formalism for the implementation of the two approaches. Section 3 is devoted to the presentation of the numerical results. There, we study the role played by different parameters: the integrated density of states, the velocity and the spatial decay rate of the perturbations. In the last section, we summarize the main results and briefly discuss the open problems.

2. Theory

We start by introducing the model of coupled maps that will be our reference system throughout the entire paper,

$$y^i_{t+1} = f\left[(1-\varepsilon)y^i_t + \frac{\varepsilon}{2}\left(y^{i-1}_t + y^{i+1}_t\right)\right], \qquad (1)$$

where $i = 1, \ldots, L$ and t are spatial and temporal (integer) indices, respectively, while $\varepsilon \in (0, 1)$ represents the diffusive coupling and $f(y)$ is a map of the unit interval onto itself. Let us now consider an infinitesimal perturbation δy^i_t, initially localized in a finite region of length $M + 1 \ll L$ centred around the origin ($\delta y^i_0 = \xi^i \Theta(M/2 - \mathrm{i})\Theta(\mathrm{i} + \mathrm{M}/2)$, where Θ is the Heaviside function and the ξ^is are iid random variables). The standard CLE is defined as

$$\Lambda(v, 0) = \lim_{t\to\infty} \frac{1}{t} \log \frac{\left|\delta y^{vt}_t\right|}{\left|\delta y^0_0\right|}, \qquad (2)$$

where the '0' in parentheses signifies that we refer to the maximum exponent. The formula can be easily extended to generic dynamical systems, by replacing the absolute value $|\delta y^i_t|$ with any norm quantifying the amplitude of the perturbation on the site i at time t. Equation (2) deals with the local amplitude of the perturbation, but does not tell anything about the way it fills the tangent space in the many directions around the reference trajectory. In order to address this issue, it is necessary to explore the spatial structure of the perturbations. In the computation of the maximal CLE, it is sufficient to let *one* perturbation evolve freely in the space and, afterwards, to focus the attention on its amplitude along specific world lines ($i = vt$). Willing to go beyond the maximal CLE, one is forced to consider a set of localized (but linearly independent) initial conditions. A natural idea would be that of: (i) considering $M + 1$ perturbations in a sufficiently large lattice; (ii) letting them freely expand over the entire space; (iii) orthogonalizing them [9] within a (moving) window of fixed size $(M + 1)$. Unfortunately, as shown in [7] for a static window, this naive approach corresponds *de facto* to computing the first $M + 1$ exponents in a system of size $M + 1 + 2t$ [6], i.e. an increasingly small fraction $n = (M + 1)/(M + 1 + 2t)$ of the entire spectrum, which eventually reduces to the maximum exponent (for each specific velocity). Accordingly, a theoretical and practical

[6] The size of the effective region covered by the perturbations grows with a velocity slower than $v = 1$ on each side, but this does not affect the general argument.

difficulty emerges: defining a strategy that avoids the convergence towards the same (maximally expanding) direction. One way out consists not only in restricting the orthogonalization to a moving window (of size $L_w \leqslant M+1 \ll L$), but also in the evolution itself of the perturbations, with the help of suitable boundary conditions. This idea, which was already suggested in [8], is not the optimal solution, as the initial perturbations do not evolve freely; artificial modifications have to be introduced on the boundaries to confine the evolution within the prescribed window. Nevertheless, since it turns out that boundary conditions do not matter for large enough L_w (see below), we can at least claim that the approach makes sense.

Let us now be more specific and explain how the LE can be determined in a frame that moves with a generic velocity v in a discrete spatio-temporal lattice. We introduce two types of 'moves' in tangent space: the first corresponds to a static window (**0**), and the second to a right-shift by a single site (**1**, without loss of generality we discuss only windows moving to the right). The corresponding rules are

$$\delta y_{t+1}^{k} = m_t^i \left[\frac{\varepsilon}{2} \delta y_t^{j-1} + (1-\varepsilon) \delta y_t^j + \frac{\varepsilon}{2} \delta y_t^{j+1} \right], \tag{3}$$

where $1 \leqslant k \leqslant L_w$ denotes the position within the moving window, while i denotes the absolute position in the lattice and $m_t^i = f'\big[(1-\varepsilon) y_t^i + \varepsilon\big(y_t^{i-1} + y_t^{i+1}\big)/2\big]$. 0- and 1-moves correspond to $j = k$ and $j = k+1$, respectively. The restriction of the rule to a finite interval requires extra assumptions for $\delta y_t^{L_w+1}$ and δy_t^0 ($\delta y_t^{L_w+2}$), to close the model for a 0 (1) move. We have typically worked by assuming all of them to be equal to zero, but we have initially verified that the same results are obtained also for different choices (e.g., $\delta y_t^0 = \delta y_t^1$). As a last detail, it is necessary to specify the sequence of **0**s and **1**s that is used to study the velocity v. Given that v is obviously equal to the fraction of 1s, several options are *a priori* possible. The velocity $v = 2/5$ can be, for instance, generated either with the sequence **0100 101 001** ... or **0001 100 011** .... One can verify that the different choices yield (slightly) different results: this is because the operations associated with the two moves do not commute. A uniform motion in the space–time (i, t) is identified by the straight line $i = vt$. Since **0** (**1**) identifies the move $(i, t) \to (i, t+1)$ ($(i, t) \to (i+1, t+1)$), the optimal sequence of symbols is the one which corresponds to a path in the lattice of integer pairs (i, t) that deviates the least from (t, vt). This corresponds to the most uniform distribution of **0** and **1**s (i.e **0100 101 001** ..., for $v = 2/5$). Note that this would be less of a problem in continuous space–time systems, as one can, in principle, select arbitrarily small time- and space-steps. As a result, for any given velocity v, we can determine the whole spectrum $\Lambda(v, n)$, where $n = l/L_w$ and l means that we refer to the lth largest exponent. From now on, we refer to this method as the *direct* one.

An alternative approach consists in considering the evolution of a perturbation with an exponential profile, namely $\delta y_t^i = \Phi_t^i e^{-\mu i}$. This requires studying the evolution equation

$$\Phi_{t+1}^{i} = m_t^i \left[\frac{\varepsilon}{2} e^{\mu} \Phi_t^{i-1} + (1-\varepsilon) \Phi_t^i + \frac{\varepsilon}{2} e^{-\mu} \Phi_t^{i+1} \right], \tag{4}$$

where $i = 1, \ldots, L$, while periodic boundary conditions are assumed to hold for Φ_t^i. By solving the model (4) for different values of μ, one obtains the temporal spectrum $\lambda(n, \mu)$.

We claim that the convective Lyapunov spectrum can be obtained by a Legendre transform of $\lambda(n, \mu)$,

$$\Lambda(v, n) = \lambda(n, \mu) - \mu v, \tag{5}$$

where $v = d\lambda/d\mu$ (and the set of transformations is completed by the symmetric expression $\mu = -d\Lambda/dv$). Altogether, equation (5) extends to finite n the transformation initially proved for $n = 0$ [4]. Its original justification is based on the observation that the profile of an initially localized perturbation is, at time t, locally exponential with a decay rate μ that depends on the position $i = vt$. For $n > 0$, it is not clear which profile one should refer to. For this reason, the above definition is essentially a formal one.

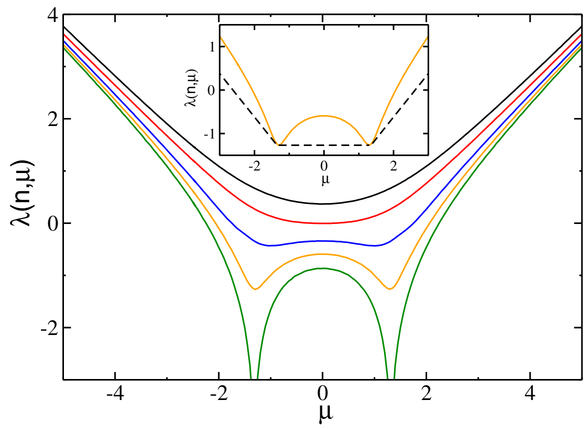

Figure 1. Temporal Lyapunov exponents $\lambda(n, \mu)$ versus μ for a chain of $L = 100$ coupled logistic maps with $r = 4$ and $\varepsilon = 1/3$. From top to bottom, the curves refer to $n = 0$, 0.5, 0.75, 0.9 and 1. The inset contains the Maxwell construction (see the dashed straight lines), for the curve corresponding to $n = 0.9$, used for the Legendre transform, as discussed in the text.

3. Numerical results

We have tested both approaches by studying a chain of coupled logistic maps, i.e. with $f(y) = ry(1 - y)$ ($r = 4$), $y \in [0; 1]$ and $\varepsilon = 1/3$ (these are the same parameter values adopted in [8]).

In figure 1, we plot the temporal spectra for $L = 100$[7] and some values of n (namely, $n = 0$, 0.5, 0.75, 0.9 and 1). We have also verified that L is large enough to ensure the thermodynamic limit. The uppermost curve corresponds to the maximum exponent that is known to grow monotonously for increasing (in absolute value) μ. On the other hand, the lowermost curve, which corresponds to the minimum LE, is not only non-monotonous, but also exhibits even a singular behaviour for $|\mu| \approx 1.31$.

3.1. Convective exponents versus velocity

In figure 2(*a*), we plot the convective spectra obtained by Legendre transforming two of the curves reported in figure 1. The upper solid curve is the standard convective spectrum. It starts from a maximum value for $v = 0$ that corresponds to the usual maximum LE and crosses the zero axis at $v_c = 0.510(5)$ which indicates the maximal propagation velocity of (infinitesimal) perturbations. The lower solid curve corresponds to $n = 0.5$ and the very fact it is nearly zero for $v = 0$ indicates that approximately half of the standard LEs are positive.

In order to check the equivalence between the direct and the chronotopic approaches, we have computed the convective spectra also by iterating localized perturbations, implementing the method described in the previous section. The (orange) asterisks in figure 2(*a*) correspond to the outcome of simulations performed with $L_w = 100$. The agreement is rather poor and even gets worse upon increasing the window size L_w (not reported). However, we discovered that the problem is not conceptual, but numerical. The reason is that the Lyapunov vectors in the moving windows are exponentially localized around the left border of the window.

[7] Note that in the chronotopic approach the relevant scaling parameter is the actual system size L, while in the direct approach it is the size L_w of the moving window.

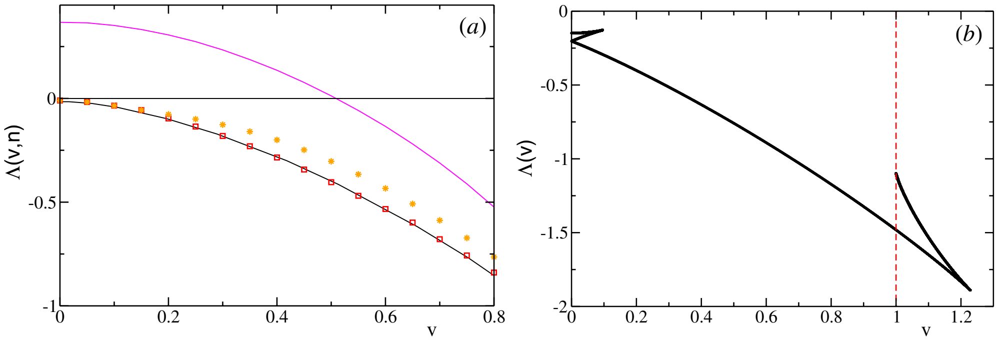

Figure 2. Convective exponents $\Lambda(v, n)$ versus the velocity of the comoving reference frame for logistic (*a*) and Bernoulli (*b*) coupled map lattices. (*a*) The convective exponents have been obtained for $n = 0$ (upper curve) and $n = 0.5$ (lower curve). The solid lines have been generated by Legendre transforming (see equation (5)) the curves reported in the previous figure. The symbols correspond to the direct estimates of the convective exponents in double precision for $n = 0.5$ and $L_w = 100$: (orange) asterisks refer to $\gamma = 0$, while (red) squares to $\gamma = 1.0$. (*b*) The reported convective spectrum has been analytically determined by performing the Legendre transform of equation (7) for $n = 0.75$ and $L = 100$.

Accordingly, many of their components are so small that double-precision accuracy (i.e. with 14-15 digits) is not sufficient, especially for large values of L_w. As a matter of fact we have verified that by employing extended precision (i.e. with approximately 30 digits) the agreement increases. However, an even better agreement can be obtained already with double precision, by introducing a weighted Euclidean norm. More precisely, given any two vectors $\mathbf{u} = \{u^i\}$, $\mathbf{v} = \{v^i\}$, we define the scalar product as

$$\mathbf{u} \cdot \mathbf{v} = \sum_i u_i v_i \, e^{\gamma i}, \tag{6}$$

where γ is a free parameter (the standard definition corresponds to $\gamma = 0$) [8]. By comparing extended precision with double precision for different γ values, we concluded that $\gamma = 1$ is a nearly optimal choice (see the red squares in figure 2(*a*) which agree pretty well with the outcome of the chronotopic approach). However, a proper selection of γ does not completely solve the problem: for large velocities and larger values of L_w, numerical accuracy remains an issue.

The relevant message that comes from the numerical analysis is that the definition of convective Lyapunov spectra through the chronotopic approach is not simply formal but provides the correct answer and, moreover, the method is by far more reliable than the direct one, since one does not face numerical inaccuracy issues. Incidentally, the comparison between the two approaches has allowed discovering the serious problems of numerical accuracy that affect the direct approach and thereby the simulations reported in [8]. Let us finally note that the zero-velocity convective Lyapunov $\Lambda(0, n)$ coincides with the standard LE for the same density (i.e. the temporal LE $\lambda(n, \mu)$ for $\mu = 0$). This property essentially means that in an open system the volume growth rate, measured locally where the perturbation has been created, coincides with the usual growth rate as defined in closed systems. We will see that this *natural* equivalence does not hold for larger densities.

[8] Lyapunov exponents are independent of the norm, i.e. of γ, but this is strictly proven only for finite-dimensional systems. In a case like the present one, where the thermodynamic limit is considered, one cannot exclude problems due to the non-commutativity with the infinite-time limit that is implicit in the definition of the LEs.

Upon increasing n, the changes of concavity and even the lack of monotonicity of $\lambda(n, \mu)$ lead to the emergence of extra branches in the convective spectrum, as shown in figure 2(b), where we report the spectrum for Bernoulli maps ($f(x) = 2x \bmod(1)$ with $\varepsilon = 1/3$), since the curve can be determined analytically. On the one hand, the multistability observed at small velocities is a consequence of the fact that $\lambda(n, \mu)$ becomes a local maximum for $\mu = 0$, rather than an absolute minimum as for lower densities. On the other hand, the coexistence of two solutions for $v > 1$ follows from the asymptotically different concavity of $\lambda(n, \mu)$ for $\mu \gg 1$.

In this case, statistical mechanics suggests that one construct the maximum convex hull which encircles from below the entire curve $\lambda(n, \mu)$ (from $\mu = +\infty$ to $\mu = -\infty$). The procedure is exemplified in the inset of figure 1 for $n = 0.9$. As the first step, the two minima $\pm\bar{\mu}$ of $\lambda(n, \mu)$ are connected by a horizontal line. This implies that in the interval $[-\bar{\mu}, \bar{\mu}]$, $v = \mathrm{d}\lambda/\mathrm{d}\mu \equiv 0$. Next, in order to get rid of the inflection points to the right (left) of $\bar{\mu}$ $(-\bar{\mu})$, it is necessary to prolong $\lambda(n, \mu)$ starting from the point where its slope is equal to 1 (-1) (see the two additional dashed lines in the inset of figure 1). As a result, the zero-velocity CLE does not coincide with the growth rate of a flat profile (i.e. to $\mu = 0$), but rather with the growth rate of an exponentially localized profile (with an exponent $\mu = \bar{\mu}$). In other words, the only physically meaningful branch in figure 2(b) is the lowermost one, which corresponds to $\mu \geqslant \bar{\mu} > 0$. In the following, we indeed show that the direct method selects the lowest branch. The most relevant consequence is that the zero-velocity CLE $\Lambda(0, n)$, which is now associated with a finite μ-value, is strictly smaller than the corresponding usual LE $\lambda(n, 0)$ (associated with a flat perturbation). This result follows from the opposite concavity of $\lambda(n, \mu)$: exponential profiles grow slower than the flat one, which thus becomes unstable in the free propagation of initially localized perturbations. As a result, the maximal rate observed for the propagation in an open system is attained for the μ value that corresponds to the minimum of $\lambda(n, \mu)$ (for the given n value). One can altogether attribute this phenomenon to strong convective mechanisms that spoil the local perturbation growth.

On the other hand, the convex-hull construction for $\mu > \bar{\mu}$ implies that the branch to the right of $v = 1$ has to be removed (and, analogously, the one to the left of $v = -1$). This truncation has a natural physical interpretation as it corresponds to discard 'superluminal' velocities, i.e. those that are greater than the maximal allowed propagation velocity in a chain of maps with nearest-neighbour coupling. Mathematically, it originates from the fact that the limit velocity corresponds to the asymptotic slope of $\lambda(n, \mu)$ versus μ, which is known to be equal to 1 in this physical setup [3].

3.2. Convective exponents versus density

Now, instead of looking at the dependence of a generic CLE on the velocity, we look at the shape of the convective spectra at given velocities, as this helps to clarify the phenomenology observed at large integrated densities. An example is reported in figure 3(a) for $v = 1/5$. Above a certain density n_c, the spectrum obtained via the Legendre transform displays three different branches: the lower one is associated with positive μ-values, while the other two with negative μ. Once again the standard direct estimates suffer problems of numerical accuracy (see the upper solid curve in figure 3(a)). The improved simulations (for $\gamma = 2$) seem to converge towards the lower branch, but there is still some discrepancy and it is difficult to decide whether this is due to finite-size corrections.

In order to obtain more convincing evidence, we have decided to consider a chain of Bernoulli maps. Since the multipliers are constant in space and time, we expect smaller finite-size corrections and, moreover, the estimation of the convective spectra is simpler,

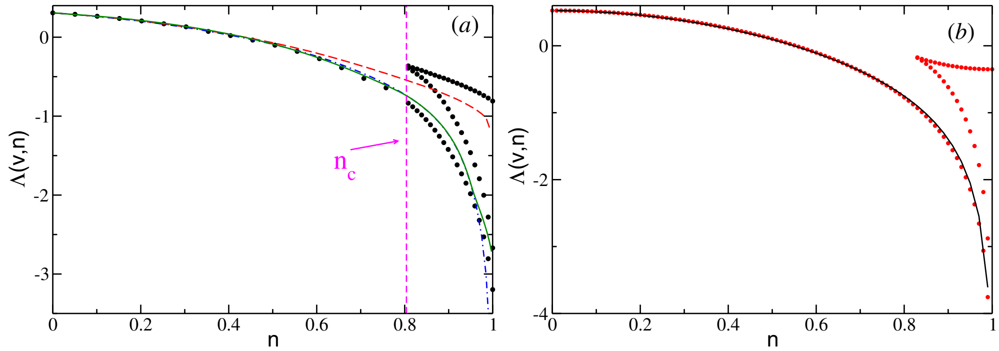

Figure 3. Spectrum of the convective exponents $\Lambda(v, n)$. (*a*) Coupled logistic maps for $v = 1/5$. The solid lines correspond to direct measurements. From top to bottom: $L_w = 100$ and $\gamma = 0$ (red dashed line), $L_w = 200$ and $\gamma = 2$ (blue dot–dashed line) and $L_w = 100$ and $\gamma = 2$ (green solid line). Full circles correspond to the Legendre transform for $L = 100$. Finally, the vertical dot–dashed (magenta) line indicates the n_c-value. (*b*) Bernoulli maps for $v = 1/3$, estimated analytically via the Legendre transform (red circles) and directly by diagonalizing a constant 50×50 matrix (solid line) with extended precision.

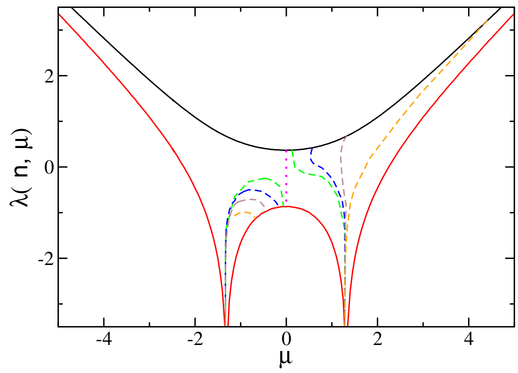

Figure 4. Isolines in the plane (λ, μ) corresponding to a constant velocity v for coupled logistic maps. The vertical dotted line refer to $v = 0$, while the other dashed lines from left to right for $\mu > 0$ (resp. right to left for $\mu < 0$) correspond to $v = 0.05$, 0.20, 0.50 and 0.95 with $L = 100$.

as it reduces to the diagonalization of a matrix (for rational velocities). In fact, in this model, the tangent matrices depend only on the type (0 or 1) of move. Therefore, given a rational velocity, characterized by a periodic sequence of 0s or 1s (with period P), it is sufficient to multiply P of such matrices and thereby determine the eigenvalues. The results for $v = 1/3 = (001\,001\,001\ldots)$ are reported in figure 3(*b*) and confirm that the direct method selects the lower branch (the agreement is already quite impressive for a window of size $L_w = 50$). Additional insight can be gained by plotting the paths in (λ, μ)-plane that correspond to spectra with different velocities (see figure 4). They are the isolines where the slope $d\lambda/d\mu = v$ stays constant. The vertical line at $\mu = 0$ is the path for the standard Lyapunov spectrum. For finite velocities, the line breaks into two components that lie in the positive and negative μ half-planes, respectively: the former one corresponds to the lower branch in figure 3, while the latter one gives rise to the two upper branches.

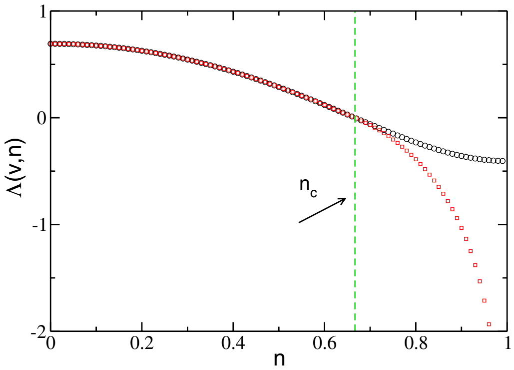

Figure 5. Spectrum of the convective exponents $\Lambda(v, n)$ for coupled Bernoulli maps for $v = 0$ (circles) and $v = 0.001$ (squares), estimated by Legendre transforming of equation (7). The parameters are $a = 2$ and $\varepsilon = 1/3$.

A moment's reflection suggests that the mathematical origin of the multiple branches seen in figure 4 is the change of concavity of $\lambda(n, \mu)$ (as a function of μ) upon increasing n: it suddenly enforces points with positive derivative to jump from the right to the left side of $\mu = 0$. Once again the Bernoulli maps allow for an accurate investigation.

The expression for the temporal exponent is [3]

$$\lambda(n, \mu) = \log a + \tfrac{1}{2} \log |(1 - \varepsilon)^2 + 2\varepsilon(1 - \varepsilon)(\cosh \mu) \cos \pi n + \varepsilon^2(\cosh^2 \mu - \sin^2 \pi n)|. \tag{7}$$

By expanding this expression for small μ values, it is easy to verify that the quadratic term in μ changes sign for

$$n = n_c \equiv 1 - \frac{\operatorname{acos}[\varepsilon/(1 - \varepsilon)]}{\pi}, \tag{8}$$

provided that $\varepsilon < 1/2$. We have estimated the spectrum of the convective exponents for $v = 0$ and $v = 0.001$. In figure 5, one can appreciate that for $n < n_c$, they are nearly identical, while for $n > n_c$, they separate out by a finite amount, as a result of the selection of the lower branch.

4. Conclusions and open problems

We have shown that the notion of the convective Lyapunov exponent can be extended from the maximum to an entire spectrum. The comparison between two different methods reveals a complex scenario with a transition to multiple branches which we attribute to the competition between diffusive and convective mechanisms. Below a critical dimension density n_c, the scenario is similar to that observed for the maximum convective exponent. In particular, $\lambda(n, 0)$ coincides with the zero-velocity CLE $\Lambda(0, n)$, which is a standard quadratic maximum of $\Lambda(v, n)$ (for fixed integrated density n). Above $n = n_c$, the maximum of $\Lambda(v, n)$ is no longer quadratic (left and right derivatives differ from zero) and $\Lambda(0, n) < \lambda(n, 0)$, indicating that initially localized perturbations grow slower than the generic uniform ones (as quantified by the standard Lyapunov spectra). This phenomenon is the consequence of a change of concavity of the chronotopic Lyapunov spectra. In the case of Bernoulli maps, it has been possible to determine an analyitic expression for n_c, and preliminary studies indicate that the same scenario arises also in chains of Stuart–Landau oscillators [10].

As the very existence of n_c follows from a general property of the chronotopic Lyapunov spectrum (a change of its concavity along the μ axis), n_c is a dynamical invariant, analogously to the fraction of positive Lyapunov exponents and the Kaplan–Yorke dimension. The existence of a critical density n_c suggests that the evolution of the most stable modes (those which correspond to larger values of the density n) is controlled by convective rather than diffusive processes. The physical consequences of this different scenario remain, however, unclear and require further study.

It is, nevertheless, natural to ask about the universality of the transition. In the Bernoulli map, we have seen that if $\varepsilon > 1/2$, then all temporal Lyapunov exponents exhibit a minimum for $\mu = 0$ and no transition arises. It would be extremely interesting to find either physical models where all temporal Lyapunov exponents exhibit a maximum or to prove that this scenario is conceptually impossible because of some general physical principles.

Finally, we wish to remind the reader that the 'direct' definition of convective Lyapunov spectra is partially unsatisfactory, as it requires in-principle-unnecessary boundary conditions. An open system approach such as that developed in [7] would be much more appealing, but it requires incorporating the additional parameter $g = T/L$ in the current theory.

An alternative idea could be that of referring to covariant Lyapunov vectors [11]: if one could indeed 'build' the initial perturbation by using only such vectors, then one would be automatically assured that no more unstable degrees of freedom are going to be excited. There is, however, a practical problem: the measurement of asymptotic quantities would require one to evolve back and forward the chain on sufficiently long timescales to allow the perturbation to propagate over sufficiently large distances.

Acknowledgments

AKJ undertook this work with the support of the ICTP 'Programme for Training and Research in Italian Laboratories' (TRIL), Trieste, Italy. AT acknowledges the Villum Foundation for partial support received during his visit to the Department of Physics and Astronomy of the University of Aarhus (Denmark).

References

[1] Manneville P 1985 *Macroscopic Modeling of Turbulent Flows* (*Lecture Notes in Physics* vol 230) ed U Frisch *et al* (Berlin: Springer) p 319
Livi R, Politi A and Ruffo S 1986 *J. Phys. A: Math. Gen.* **19** 2033
Grassberger P 1989 *Phys. Scr.* **40** 346
[2] Deissler R J and Kaneko K 1987 *Phys. Lett.* **119** 397
[3] Lepri S, Politi A and Torcini A 1996 *J. Stat. Phys.* **82** 1429
Lepri S, Politi A and Torcini A 1997 *J. Stat. Phys.* **88** 31
Lepri S, Politi A and Torcini A 1997 *Chaos* **7** 701
[4] Politi A and Torcini A 1994 *Europhys. Lett.* **28** 545
[5] Huerre P and Monkewitz P A 1990 *Annu. Rev. Fluid. Mech.* **22** 473
[6] Sandstede B and Scheel A 2000 *Physica* D **145** 233
[7] Cipriani P and Politi A 2004 *J. Stat. Phys.* **114** 205
[8] Mayer-Kress G and Kaneko K 1989 *J. Stat. Phys.* **54** 1489
[9] Shimada I and Nagashima T 1979 *Prog. Theor. Phys.* **61** 1605
Benettin G, Galgani L, Giorgilli A and Strelcyn J M 1980 *Meccanica* **15** 21
[10] Kenfack Jiotsa A, Politi A and Torcini A 2011 unpublished
[11] Ginelli F, Poggi P, Turchi A, Chaté H, Livi R and Politi A 2007 *Phys. Rev. Lett.* **99** 130601